

An Aluminum/Graphite Battery with Ultra-High Rate Capability

Giuseppe A. Elia,^{*[a]} Neil A. Kyeremateng,^[a] Krystan Marquardt,^[a] and Robert Hahn^[b]

A high-performance Al/graphite battery has been investigated, employing a natural graphite cathode (NG) and 1-ethyl-3-methylimidazolium chloride (EMIMCl):AlCl₃ as electrolyte. The employed graphite is characterized by excellent reversibility as revealed by electrochemical tests and ex-situ XRD. The Al/EMIMCl:AlCl₃/NG battery showed extraordinary performance in terms of rate capability, and cycle life. The cell delivered a capacity of 110 mAh g⁻¹ at lower current values, retaining 90% and 60% of the capacity employing a current of 20 Ag⁻¹ and

50 Ag⁻¹, respectively (i.e., a complete charge-discharge cycle in 35 and 9 seconds, respectively). Furthermore, the cycling test performed using a current of 20 Ag⁻¹ revealed an extremely long calendar life of half million of cycles. The practical applicability of the investigated Al/graphite system has been ascertained; this involved estimating the energy efficiency as a function of current rate and carefully calculating the practical energy densities that can be obtained from the system.

1. Introduction

The development of sustainable electrochemical storage systems is very important for allowing the penetration in the electric grid of renewable energy production and for electric mobility. In particular, batteries play an important role in electric mobility, and are essential for the storage of electricity produced from renewable sources like wind and solar. Among the battery systems, lithium-ion batteries (LIBs) are those with the highest energy density, for that reason they are the power source of choice for EVs.^[1–8] Nevertheless, due to the limited resource of lithium, and of the transition metals (Co in particular) used for the realization of the battery, the long-term sustainability of such system is questioned.^[9] In order to tackle this issue the diversification of electrochemical storage systems constitute a viable route as a consequence energy storage systems using abundant elements such as Na,^[10–14] K,^[15–17] Ca,^[18,19] Mg,^[20,21] and Al^[22–24] are receiving significant attention. In particular, aluminum characterized by a volumetric capacity of 8040 mAh cm⁻³, and a gravimetric capacity of 2980 mAh g⁻¹ is considered an appealing candidate for the realization of sustainable batteries. In fact, aluminum is the most abundant metal element in the earth's crust. Accordingly, several research groups worldwide have investigated various aluminum battery configurations. Among them, those using graphite cathode^[25–35] showed the best cycle life and rate capability. As a matter of fact, recently, Jiao et al.,^[36] reported an Al/graphite battery prototype suitable for practical applications. Several research efforts have been focused on the synthesis of certain

graphite morphologies to improve the electrochemical performance of the system, including 3D graphitic foam, 3D graphene mesh, etc.^[28,29,33] Herein, we demonstrate that superior performances can be obtained by simply using commercial natural graphite as the cathode material. The electrochemical behavior of the NG cell has been compared with the conventional pyrolytic graphite (PG) cathode used as a benchmark.^[27,37] The developed Al/EMIMCl:AlCl₃/NG cell showed extraordinary performance in terms of rate capability, and cycle life. The investigated cell is capable to retain the 90% and 60% of the nominal capacity (110 mAh g⁻¹), employing respectively a current of 20 Ag⁻¹ and of 50 Ag⁻¹, i.e., a complete charge-discharge cycle in 35 and 9 seconds, respectively. Finally, the practical applicability of the investigated Al/NG system has been ascertained; this involved estimating the energy efficiency as a function of current rate and calculating the practical energy densities that can be obtained from the system. In particular, for the latter, it has been evidenced that, due to the nature of the electrochemical process leading to the depletion of the AlCl₄⁻ anion from the electrolyte during the charge process, the electrolyte has an enormous contribution to the mass and the volume of the Al/graphite cell. The study also evidenced that the concentration of the AlCl₃ salt in the electrolyte solvent has a greater influence on the attainable energy density of the Al/NG system in comparison to the capacity that can be delivered by the graphite material.

2. Results and Discussion

Figures 1a-b report the voltammograms of the second cycle of the cyclic voltammetry performed using the Al/EMIMCl:AlCl₃/NG cell (Figure 1a) and the Al/EMIMCl:AlCl₃/(PG) cell (Figure 1b) at a scan rate of 0.1 mV s⁻¹. The voltammogram of the cell employing the NG electrode evidences the presence of five sharp, symmetric peaks during the anodic scan, which are perfectly reversed in the cathodic scan, indicating the good reversibility of the electrochemical process taking place as a multistage anion intercalation

[a] Dr. G. A. Elia, Dr. N. A. Kyeremateng, K. Marquardt
Technische Universität Berlin
Research Center of Microperipheric Technologies
Gustav-Meyer-Allee 25, D-13355 Berlin, Germany
E-mail: elia@tu-berlin.de

[b] Dr. R. Hahn
Fraunhofer-Institut für Zuverlässigkeit und Mikrointegration
Gustav-Meyer-Allee 25, D-13355 Berlin, Germany

 Supporting information for this article is available on the WWW under <https://doi.org/10.1002/batt.201800114>

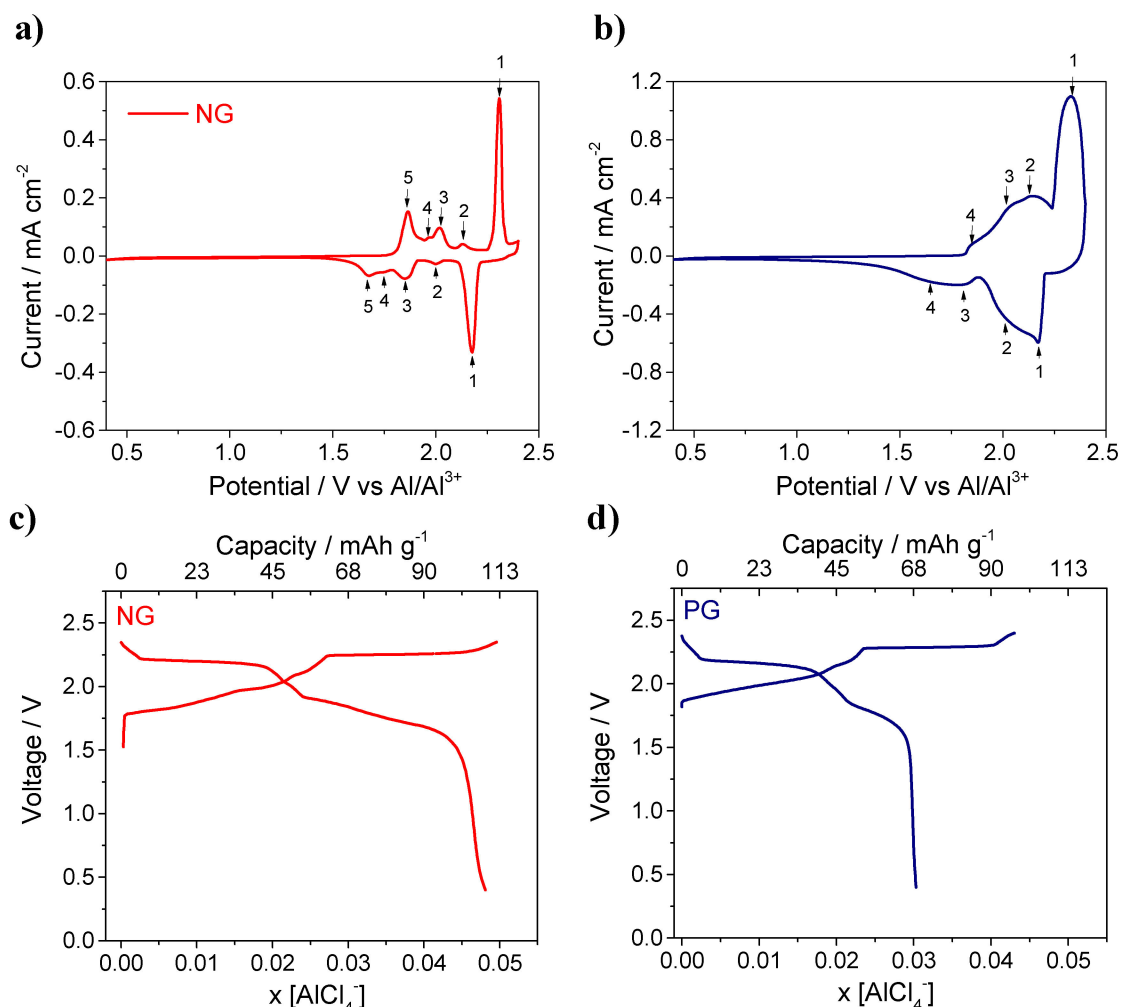
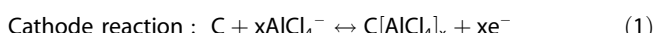


Figure 1. Second cycle cyclic voltammograms of (a) Al/EMIMCl:AlCl₃/NG cell and (b) Al/EMIMCl:AlCl₃/PG cells at a scan rate of 0.1 mV s⁻¹. First cycle voltage profile of (c) Al/EMIMCl:AlCl₃/NG cell and (d) Al/EMIMCl:AlCl₃/PG cells after galvanostatic cycling with 50 mA g⁻¹ current, at 25 °C. The voltage profiles are reported vs the x mole of AlCl₄⁻ intercalated for each mole of carbon.

within the graphite layers.^[23,38] On the contrary, the voltammogram of the Al/EMIMCl:AlCl₃/PG cell (Figure 1b), reveals only four broad and asymmetric peaks. The broadening of the peaks indicates a kinetically limited electrochemical process in the PG electrode as compared to the NG electrode. Figures 1 c-d show the voltage profiles of the first cycles of the galvanostatic cycling tests performed on the Al/EMIMCl:AlCl₃/NG (Figure 1c) and the Al/EMIMCl:AlCl₃/PG cells (Figure 1d) at 50 mA g⁻¹. For each cell, the voltage profile is reported as a function of the degree of intercalation of the anion ($x_{\text{AlCl}_4^-}$), which can be easily calculated according to Equation (1):



For the calculation, it was assumed that for each mole of electron exchanged, an equivalent mole of AlCl₄⁻ is intercalated in the graphite. This assumption is well supported by literature results, indicating that the AlCl₄⁻ is the anionic specie

intercalated within the graphite planes.^[23,27,33,35,39] Figure 1c evidences that, at full charge, the NG intercalates 0.05 mole of AlCl₄⁻ for each mole of carbon (i.e., 110 mAh g⁻¹ capacity), obtaining a C[AlCl₄]_{0.05} GIC. As shown in Figure 1c, the discharge capacity was also very comparable to the charge capacity, which is an indication of excellent coulombic efficiency and a fully reversible electrochemical process. On the contrary, the PG cell seems to react only with $x_{\text{AlCl}_4^-}$ of 0.045 (100 mAh g⁻¹ capacity) upon full charge, and the stored charge could not be fully recovered at the end of the discharge process; this is indeed an indication of partially irreversible electrochemical process in the PG material. This phenomenon has already been investigated by our group, evidencing that the PG's first-cycle irreversibility is associated to the retention of some of the AlCl₄⁻ anions intercalated in that type of graphite material.^[27]

Figures 2a shows the ex-situ XRD patterns of the pristine, the fully charged, and fully discharged NG electrodes. Upon full charging, the diffractogram reveals the disappearance of the main (002) graphitic reflection and the appearance of two new

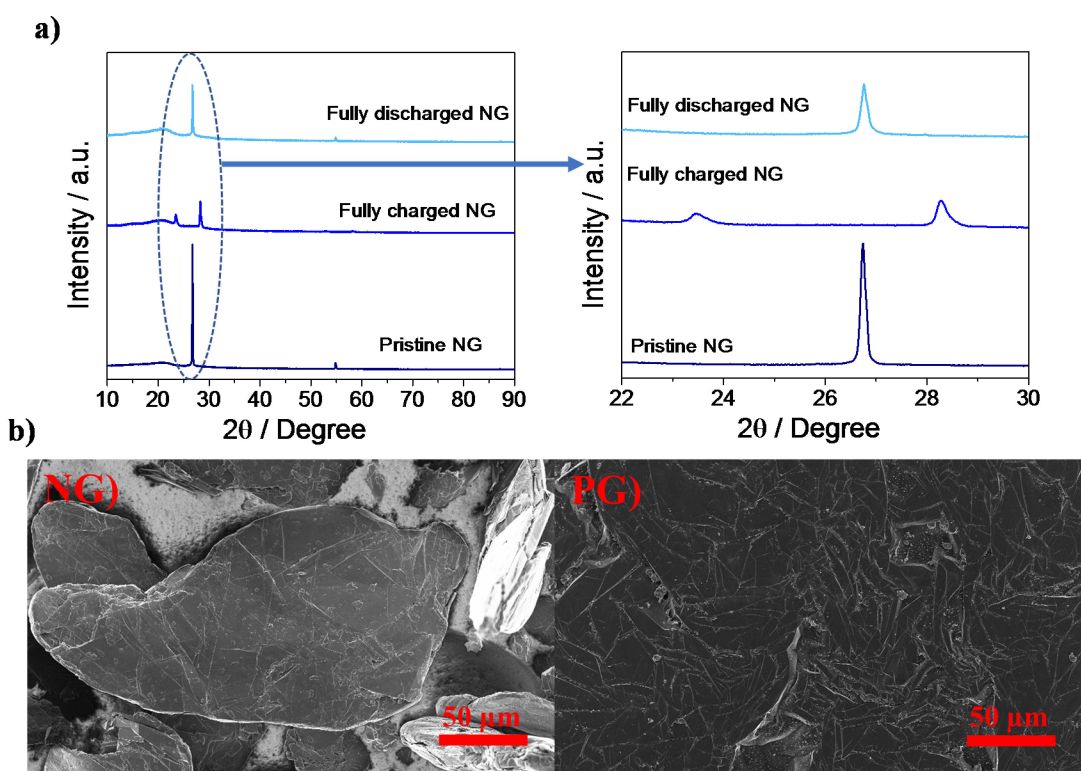


Figure 2. (a) Ex-situ X-ray diffractograms of pristine, fully charged and fully discharged NG electrodes. Magnification of the 22° – 30° 2θ angle regions. (b) SEM images of the PG and the NG materials.

reflections, indicating the formation of a graphite intercalated compound (GIC),^[38,40–42] due to the intercalation of the AlCl_4^- anion within the graphite layer.^[23,27] After the discharge process, the diffractogram shows the full recovery of the (002) graphitic reflection, indicating the perfect reversibility of the electrochemical process; this also means that the NG does not undergo the partial anion retention as it is the case for the PG electrode.^[23,27] The different electrochemical behaviors of the two materials in the aluminum cell cannot be ascribed to any differences in their crystal structures nor to the presence of unwanted functional groups. Figure S2a reports a comparison of the XRD patterns of the PG (blue curve) and of the NG (red curve), revealing no differences for the two materials; both materials exhibit high crystallinity as evidenced by the very narrow and intense graphite (002) reflection at 2θ of 26.5° . Similarly, the comparison of the Raman spectra of the two materials, reported in Figure S2b, reveals no relevant differences. In both samples, the intensity of the peak, at about 1363 cm^{-1} which is associated with the D band (disordered-band),^[43] is extremely low, indicating a high degree of order and crystallinity for both graphite samples; this also agrees with the XRD results.^[44] Furthermore, the elemental analysis performed on the two materials revealed that both are composed only of carbon. Actually, it seems the main difference between the two materials is their morphology. The marked difference in the morphology of the two materials can be seen in the SEM images presented in Figure 2b NG (left image) and of the PG (right image). The NG is formed by graphite flakes of 200–300 μm large and 20–40 μm thick, while the PG does not show,

as expected, any flakes or particles, revealing a highly-oriented graphite film with submicron-roughness on the surface. It is proposed that the particular structure of the PG electrode causes, upon the volumetric expansion due to the intercalation process, a great reduction of the porosity within the material, and consequently restricts access to some parts of the material, making those parts electrochemically inactive and leading to the irreversibility in the first cycle.^[37]

Figure 3 reports the galvanostatic cycling behavior of Al/EMIMCl: AlCl_3 /NG cells. The voltage profiles of the cell cycled at various current rates are presented in Figure 3a. It can be noticed that the cell is characterized by an excellent rate capability, and as expected, an increase in the cell polarization and a decrease of the delivered capacity upon increase of the current. Figure 3b shows the overall cycling behavior upon the rate capability test, revealing the good cyclability with satisfactory coulombic efficiency, particularly at higher current rates; this also confirms the good electrochemical stability of the investigated cell chemistry. The lower columbic efficiencies upon increasing currents can, most likely, be ascribed to a kinetic limitation of side reactions. The reported performances are really impressive, the cell still delivered 100 mAh g^{-1} of capacity employing a current of 20 A g^{-1} and 70 mAh g^{-1} with a current of 50 A g^{-1} , i.e., a complete charge-discharge cycle in 35 and 9 seconds, respectively. This characteristic is comparable to the best electrochemical supercapacitors. Figure 3c reports the results of the cycling test performed on an Al/EMIMCl: AlCl_3 /NG cell using a current of 1 A g^{-1} for 50 thousands cycles; it can be noticed that the capacity fading is nearly negligible even after

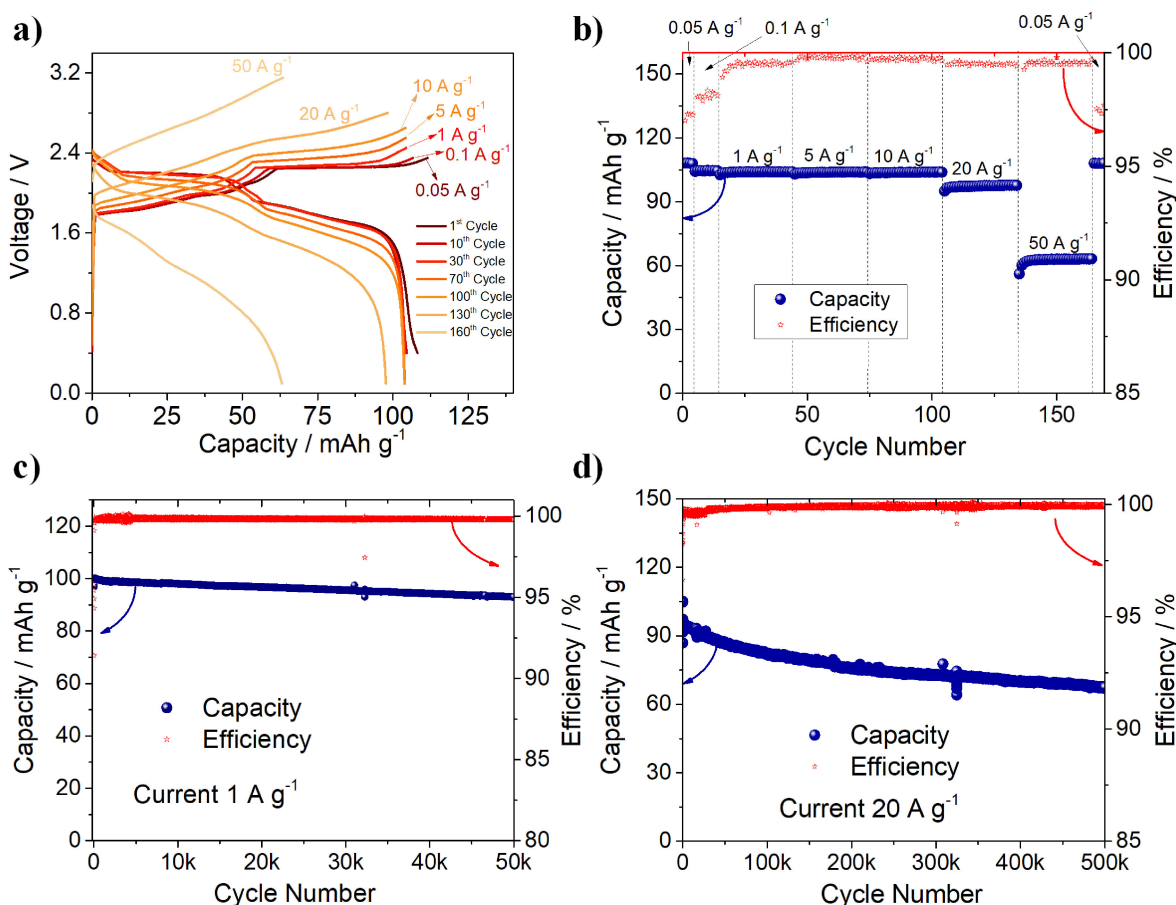


Figure 3. Electrochemical performance of Al/EMIMCl:AlCl₃/NG cells subjected to galvanostatic cycling protocols at 25 °C. (a) Voltage profiles at various current densities (0.05, 0.1, 1, 5, 10, 20, 50 A g⁻¹); (b) specific charge and discharge capacities and coulombic efficiency along the whole multi-rate test protocol. Specific charge and discharge capacities and coulombic efficiency at a current density of (c) 1 A g⁻¹ and (d) 20 A g⁻¹.

such extremely long cycling test. Furthermore, the results reported in Figure 3d on the cycling test performed using a current of 20 A g⁻¹ is truly unprecedented, as it shows a capacity fading of about the 30% after half-million cycles. It is worth emphasizing that the performance demonstrated herein is rarely reported in literature (see Table S1). The extremely elevated cycling stability of the system is most likely associated to the fact that we are working within the electrochemical stability window of the electrolyte. In fact, the decomposition (reductive) process of the electrolyte associated to the reduction of the imidazolium cation takes place at potentials lower than the potential of aluminum deposition.^[22] The oxidative decomposition of the electrolyte is associated to the decomposition of the AlCl₄⁻ anion, leading to the formation of gaseous chlorine. For that reason, there is no formation of organic reaction products at the surface of the electrode that would result in an increase of the cell impedance and a decrease of the performances. Furthermore, the formed chlorine can solubilize in the electrolyte solution, and can be again reduced during the cycling of the cell, acting as a self-overcharge protection. Clearly, the formation of the chlorine gas will have an adverse impact on the safety of the system; it will definitely require extra attention in the realization of a

hermetic cell package to avoid the undesired release of the gas in the atmosphere, which is the case for all battery chemistries.

Besides the delivered capacity value, other parameters should be considered for proper evaluation and benchmarking of the Al/graphite system. Figure 4 reports the cell overvoltage and the cell energy efficiency as a function of applied current. It can be noticed from the figure that, for currents lower than (or equal to) 1 A g⁻¹ (green part), the cell overvoltage and the energy efficiency values are almost not affected by the applied current, remaining at approximately 0.2 V and 90%, respectively. At intermediate currents (yellow part: 1 < I/A g⁻¹ ≤ 10), the cell overvoltage increases, and the energy efficiency decreases till 0.4 V and 80%, respectively. For higher currents (red part: 10 < I/A g⁻¹ ≤ 100), a sharp increase of the cell overvoltage and a sharp decrease of the energy efficiency occur; this is certainly a strong indication of the non-applicability of the system at very-high currents. In particular, the 50 A g⁻¹ current seems to be really extreme, as the energy efficiency is just about 40%. On the contrary, the energy efficiency of 70% at 20 A g⁻¹ is quite acceptable. A second excellent characteristic of the investigated system is the extremely-long cycle life.

Figure S3 reports the evolution of the theoretical energy density (black dot) and theoretical power density (blue star) as

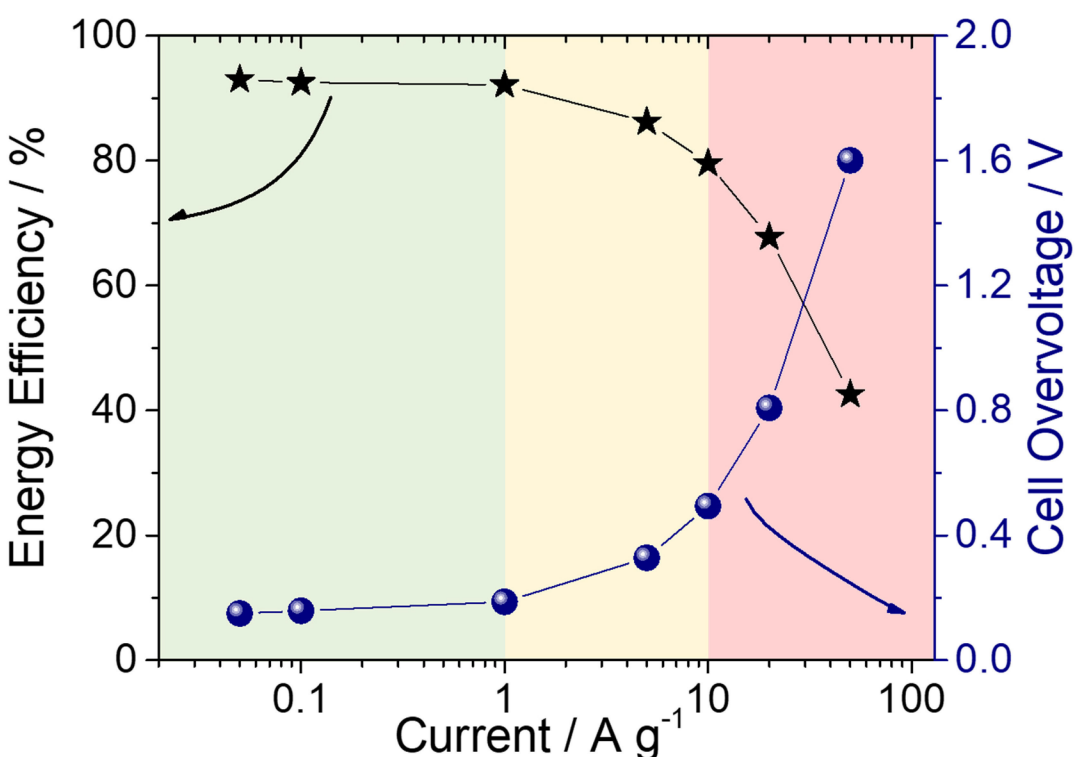


Figure 4. Average cell overvoltage (blue dot) and cell energy efficiency (black star) as a function of applied current. The x axis is in logarithmic scale. The data was obtained from the cycling test reported in Figure 2a.

function of applied current. The values are calculated from the multi-rate cycling test reported in Figure 3 considering only the graphite weight. Clearly, the values are not representative of the practical system since all the other cell components should be taken into account for the evaluation of the practical energy density of the system. The general rule of thumb, widely used for lithium-ion batteries,^[45] which considers that the practical energy/power density of the battery is of about 1/3 of the value calculated with respect to the weight of the cathode, cannot be applied in this case. In fact, in the Al/graphite system, the electrolyte is not only a media for the transport of ions but must be considered an active material. In fact, during the charge process of the battery (reaction 1) the AlCl_4^- is depleted from the solution to be inserted in the graphite electrode, inducing a variation of the electrolyte concentration. For that reason, a certain amount of electrolyte is required to keep the cell working. In order to calculate the practical performance of the system, we assumed that the EMIMCl: AlCl_3 mole ratio cannot be lower than 1, since only for mole ratios higher than 1 that the Al_2Cl_7^- species required for the reversible Al stripping/plating process (Eq. 2) is present. Assuming a capacity of 110 mAh g^{-1} with respect to the carbon mass, it is possible to calculate the amount of anion intercalated, and consequently, the amount of electrolyte required to keep the battery working within a certain mole ratio variation. In Figure S4a is reported the calculated amount of EMIMCl: AlCl_3 electrolyte required for each gram of graphite cathode, as a function of the EMIMCl: AlCl_3 mole ratio, assuming that the final mole ratio of the electrolyte reduces to 1.1 (blue star) or to 1.3 (red circle).

The graph evidences that a large amount of electrolyte is required to keep the battery working, 6 g of electrolyte are required for each gram of carbon for a cell employing the EMIMCl: AlCl_3 mole ratio of 1.5, considering that the depletion of the anion reduces the mole ratio to 1.1. The calculation indicates that for an electrolyte characterized by a higher AlCl_3 concentration, a smaller amount of electrolyte is enough. With respect to the EMIMCl: AlCl_3 mole ratio, values higher than 2 is not possible, nevertheless the use of alternatives to the EMIMCl can allow to increase the AlCl_3 concentration.^[30,32] Clearly, the elevated amount of electrolyte required to sustain the electrochemical process negatively affects the attainable energy density of the Al/graphite system. In Figure S4b is reported the trend of the attainable energy density of an Al/graphite pouch cell with respect to the EMIMCl: AlCl_3 mole ratio; the calculation was done assuming a pouch cell configuration and using the parameters listed in Table S2. The graph evidences that the energy density increases with increasing EMIMCl: AlCl_3 mole ratio, and only for extremely elevated mole ratios the energy density of the system can reach elevated values. Figure S5 shows the mass ratio (Figure S5a) and the volume ratio (Figure S5b) of an Al/graphite pouch cell considering the initial mole ratio of 2 and the final of 1.1, evidencing that major part of the mass and the volume of the battery is occupied by the electrolyte; hence, it can be emphasized that, to improve the energy density of this system, investigation on alternative electrolyte compositions capable to dissolve an elevated amount of AlCl_3 is more important than the optimization of the graphite cathode. Furthermore, due to the elevated amount of

electrolyte required, alternative cell configurations should be considered for the cell scaling up. Finally, the power and the energy densities of the investigated system are presented in the Ragone plot shown in Figure 5, to compare the electrochemical performance of the Al/graphite cell with other energy-storage systems (considering a variation of mole ratio from 2 to 1.1). The graph evidences that the theoretical energy density calculated by considering only the cathode mass, and conventionally reported in research papers, is extremely high and unrealistic. Unfortunately, this value is far from the practical one which is represented by the red star in Figure 5. It can be noticed that the realistic (attainable) energy density of the Al/graphite system is very comparable to those of Ni-MH and lead-acid batteries, but the power density is very competitive with the best-performing electrochemical supercapacitors. Furthermore, the extremely high cycle life of the system and the expected low cost, makes it appealing, especially for stationary-energy-storage applications.

3. Conclusions

A high-performance Al/graphite battery, employing natural graphite cathode and an EMIMCl:AlCl₃ electrolyte has been investigated. The employed natural graphite (NG) is characterized by an excellent reversibility as revealed by the electrochemical results. Ex-situ XRD has also been employed to confirm the complete recovery of the (002) graphite reflection upon full discharge. On the contrary, when compared to pyrolytic graphite (PG), there seems to be a partial retention of the anion in the PG's structure after the first discharge. The marked difference in the electrochemical behavior of the two materials is most likely ascribable to the different morphologies as revealed by SEM imaging, considering that XRD, Raman spectroscopy and elemental analysis did not reveal any structural or chemical differences in the two employed graphite materials. The Al/EMIMCl:AlCl₃/NG cell revealed extraordinary performance in terms of rate capability, and cycle life. The cell is characterized by a capacity retention, in respect to the 110 mAh g⁻¹ nominal capacity, of 90% with a current of 20 A g⁻¹ and 60% with a current of 50 A g⁻¹, i.e., a complete charge-discharge cycle in 35 and 9 seconds, respectively. Furthermore, the cycling test performed using a current of 20 A g⁻¹ revealed

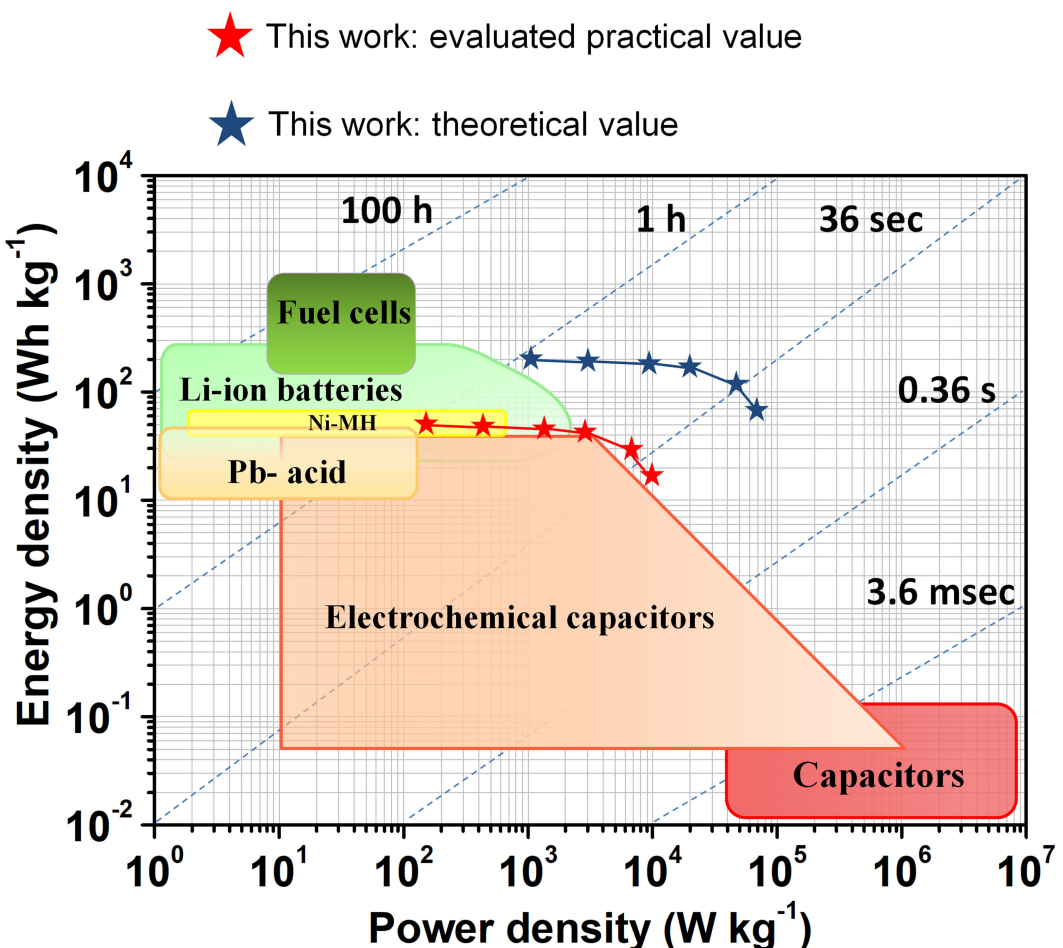


Figure 5. Ragone plot of various electrochemical energy storage systems, the blue stars represent the energy and power densities of the investigated system with respect to the carbon mass only, the red stars represent the evaluated practical energy and power densities of the system.

a really long cycle life of half-million cycles with a capacity retention of 70%. Finally, the practical applicability of the investigated Al/graphite system has been ascertained, this involved estimating the energy efficiency as a function of current rate and calculating the attainable energy densities that can be obtained from the system. Indeed, the realistic (attainable) energy density of the Al/graphite system is very comparable to those of Ni-MH and lead-acid batteries, but the power density is very competitive with the best-performing electrochemical supercapacitors. It has been demonstrated that major part of the mass and the volume of the Al/graphite system is occupied by the electrolyte; hence, to improve the energy density of this system, investigation on alternative electrolyte compositions capable to dissolve an elevated amount of AlCl_3 is more important than the optimization of the graphite cathode for better discharge capacities.

Experimental

Materials

The electrolyte 1-ethyl-3-methylimidazolium chloride:aluminum trichloride (EMIMCl): AlCl_3 in a 1:1.5 mole ratio has been provided by Solvionic. The natural graphite powder (NG) used as the cathode material was provided by PLANO GmbH. The pyrolytic graphite foil with a thickness of 100 μm and a loading of 8.6 mg cm^{-2} ^[23,27], employed as cathode material, was purchased from Panasonic.

Electrode Preparation

The preparation of the NG electrodes involved the use of Super-P C65 Imerys (SP) as conductive additive and polytetrafluoroethylene (PTFE) of 60 wt% dispersion in H_2O (3 M Dyneon™ PTFE 5032Z) as binder. The conductive additive, the binder and the NG active material were mixed together in a weight ratio of 88:10:2 (NG:PTFE:SP) using an H_2O :isopropyl alcohol mixture (8:2 volume ratio) as the solvent. Speed mixing (15 minutes) followed by sonication (5 minutes) was repeated 3 times until a homogeneous dispersion was obtained.^[46] The obtained dispersion was spray deposited on a Whatman® GF/A glass fiber separator, leading to a thick film on one side of the separator. Finally, disks of 10 mm diameter were cut and dried under vacuum at 110 °C overnight (Figure S1a).^[47] Electrodes with a loading of 4–5 mg cm^{-2} were obtained. The electrodes were directly pressed on glassy carbon current collectors rods in Swagelok®-type T-cells. This particular electrode preparation procedure has been selected due to the elevated corrosivity of the EMIMCl: AlCl_3 electrolyte, and the limited availability of suitable current collector.^[22,48] To confirm the reliability of the electrode preparation process, which has already been used for lithium-air batteries,^[47,49] the same procedure was used for the preparation of a LiFePO_4 (LFP) electrode (the LFP was kindly supplied by ALEES) with a loading of 5–6 mg cm^{-2} . Galvanostatic cycling test was done for the prepared LFP electrode with a Swagelock-type cell using lithium metal anode and a Whatman® GF/A separator soaked with LP30 electrolyte (1 M LiPF₆ in EC:DMC 1:1 vol. UBE) (Figure S1b), and the results confirmed the reliability of the electrode production process.

Physicochemical Characterization

The morphology of the NG powder and the PG foil were investigated by scanning electron microscopy (SEM) using a Zeiss Leo 1530 scanning electron microscope (SEM). The structural proprieties of the NG powder and the PG foil were investigated by X-ray diffraction (XRD) using Cu K α radiation (0.154056 nm) on a Bruker D8 Advance diffractometer in the 2 θ range from 10° to 90° with a step size of 0.01°. The cycled electrodes were fixed on the XRD sample holder in the glove box using a Kapton tape to prevent the electrodes from direct exposure to the atmosphere during the measurements. Before that, the cells were disassembled in the glovebox and the electrodes were rinsed for 30 sec in dimethyl carbonate (DMC: Sigma-Aldrich 99.9% anhydrous) to remove the residual electrolyte.^[27] Micro-Raman measurements were performed with Horiba LabRam HR800 having a laser wavelength of 488 nm with a grid of 1800, using a Renishaw with limited power and proper focusing conditions to avoid damage or modifications of the sample. Elemental analysis of the PG and the NG was performed using an EA 1110 CHNS-O Series II System.

Electrochemical Characterization

The electrochemical test were achieved employing Teflon Swagelok®-type T-cells.^[27,50] The cycling tests of Al/EMIMCl: AlCl_3 /NG cells were performed by applying increasing specific currents (from 0.05 to 50 A g^{-1}) in voltage ranges optimized for each current rate: 0.4–2.35 V for 0.05 and 0.1 A g^{-1} , 0.4–2.45 V for 1 A g^{-1} , 0.4–2.55 V for 5 A g^{-1} , 0.1–2.65 V for 10 A g^{-1} , 0.1–2.8 V for 20 A g^{-1} , 0.1–3.15 V for 50 A g^{-1} . For the long-term cycling tests, current rates of 1 A g^{-1} and 20 A g^{-1} were used. Cyclic voltammetry with a scan rates of 0.1 mV s^{-1} was also performed in the range of 2.4–0.4 V vs Al/Al³⁺.

Acknowledgements

This research was funded by the European Commission in the H2020 ALION project under contract 646286, the German Federal Ministry of Education and Research in the AISiBat project under contract 03SF0486, and the project ALIBATT under contract 03XP0128E. We acknowledge the X-ray CoreLab at Helmholtz-Zentrum Berlin for X-ray powder diffraction allocation time and support, in particular, we would like to thank Dr. Michael Tovar and Mr. Rene Gunder for their kind availability. We would like to thank Dr. Johannes Jaeschke and Dr. Astrid Gollhardt, for the support in performing the RAMAN spectroscopy measurements.

Conflict of Interest

The authors declare no conflict of interest.

Keywords: aluminium batteries • energy storage • graphite-intercalated compounds • high power density • ionic liquids

- [1] B. Dunn, H. Kamath, J.-M. Tarascon, *Science* **2011**, *334*, 928.
- [2] Z. Yang, J. Zhang, M. C. W. Kintner-Meyer, X. Lu, D. Choi, J. P. Lemmon, J. Liu, *Chem. Rev.* **2011**, *111*, 3577.
- [3] J.-J. Xu, X.-B. Zhang, *Nat. Energy* **2017**, *2*, 17133.
- [4] J.-J. Xu, Z.-W. Chang, Y.-B. Yin, X.-B. Zhang, *ACS Cent. Sci.* **2017**, *3*, 598.

- [5] Q. Cheng, Z. Song, T. Ma, B. B. Smith, R. Tang, H. Yu, H. Jiang, C. K. Chan, *Nano Lett.* **2013**, *13*, 4969.
- [6] F. Meng, H. Zhong, D. Bao, J. Yan, X. Zhang, *J. Am. Chem. Soc.* **2016**, *138*, 10226.
- [7] G. A. Elia, I. Hasa, J. Hassoun, *Electrochim. Acta* **2016**, *191*, 516.
- [8] G. A. Elia, J. Hassoun, *Solid State Ionics* **2016**, *287*, 22.
- [9] J.-M. Tarascon, *Nat. Chem.* **2010**, *2*, 510.
- [10] V. Palomares, P. Serras, I. Villaluenga, K. B. Hueso, J. Carretero-González, T. Rojo, *Energy Environ. Sci.* **2012**, *5*, 5884.
- [11] M. D. Slater, D. Kim, E. Lee, C. S. Johnson, *Adv. Funct. Mater.* **2013**, *23*, 947.
- [12] I. Hasa, D. Buchholz, S. Passerini, B. Scrosati, J. Hassoun, *Adv. Energy Mater.* **2014**, *4*, 1400083.
- [13] N. Yabuuchi, M. Kajiyama, J. Iwatate, H. Nishikawa, S. Hitomi, R. Okuyama, R. Usui, Y. Yamada, S. Komaba, *Nat. Mater.* **2012**, *11*, 512.
- [14] S. W. Kim, D. H. Seo, X. Ma, G. Ceder, K. Kang, *Adv. Energy Mater.* **2012**, *2*, 710.
- [15] Z. Jian, W. Luo, X. Ji, *J. Am. Chem. Soc.* **2015**, *137*, 11566.
- [16] W. D. McCulloch, X. Ren, M. Yu, Z. Huang, Y. Wu, *ACS Appl. Mater. Interfaces* **2015**, *7*, 26158.
- [17] X. Lu, M. E. Bowden, V. L. Sprenkle, J. Liu, *Adv. Mater.* **2015**, *27*, 5915.
- [18] A. Ponrouch, C. Frontera, F. Bardé, M. R. Palacín, *Nat. Mater.* **2015**, *15*, 169.
- [19] A. L. Lipson, B. Pan, S. H. Lapidus, C. Liao, J. T. Vaughney, B. J. Ingram, *Chem. Mater.* **2015**, *27*, 8442.
- [20] D. Aurbach, Z. Lu, A. Schechter, Y. Gofer, H. Gizbar, R. Turgeman, Y. Cohen, M. Moshkovich, E. Levi, *Nature* **2000**, *407*, 724.
- [21] D. Aurbach, G. S. Suresh, E. Levi, A. Mitelman, O. Mizrahi, O. Chusid, M. Brunelli, *Adv. Mater.* **2007**, *19*, 4260.
- [22] G. A. Elia, K. Marquardt, K. Hoeppner, S. Fantini, R. Lin, E. Knipping, W. Peters, J.-F. Drillet, S. Passerini, R. Hahn, *Adv. Mater.* **2016**, *28*, 7564.
- [23] M.-C. Lin, M. Gong, B. Lu, Y. Wu, D.-Y. Wang, M. Guan, M. Angell, C. Chen, J. Yang, B.-J. Hwang, H. Dai, *Nature* **2015**, *520*, 324.
- [24] W. Wang, Z. Cao, G. A. Elia, Y. Wu, W. Wahyudi, E. Abou-Hamad, A.-H. Emwas, L. Cavallo, L.-J. Li, J. Ming, *ACS Energy Lett.* **2018**, 2899.
- [25] H. Sun, W. Wang, Z. Yu, Y. Yuan, S. Wang, S. Jiao, *Chem. Commun.* **2015**, *51*, 11892.
- [26] L. Zhang, L. Chen, H. Luo, X. Zhou, Z. Liu, *Adv. Energy Mater.* **2017**, *1700034*.
- [27] G. A. Elia, I. Hasa, G. Greco, T. Diemant, K. Marquardt, K. Hoeppner, R. J. Behm, A. Hoell, S. Passerini, R. Hahn, *J. Mater. Chem. A* **2017**, *5*, 9682.
- [28] G. Y. Yang, L. Chen, P. Jiang, Z. Y. Guo, W. Wang, Z. P. Liu, *RSC Adv.* **2016**, *6*, 47655.
- [29] Y. Wu, M. Gong, M.-C. Lin, C. Yuan, M. Angell, L. Huang, D.-Y. Wang, X. Zhang, J. Yang, B.-J. Hwang, H. Dai, *Adv. Mater.* **2016**, *28*, 9218.
- [30] M. Angell, C.-J. Pan, Y. Rong, C. Yuan, M.-C. Lin, B.-J. Hwang, H. Dai, *Proc. Natl. Acad. Sci. USA* **2017**, *114*, 834.
- [31] W. Wang, B. Jiang, W. Xiong, H. Sun, Z. Lin, L. Hu, J. Tu, J. Hou, H. Zhu, S. Jiao, *Sci. Rep.* **2013**, *3*, 3383.
- [32] H. Jiao, C. Wang, J. Tu, D. Tian, S. Jiao, *Chem. Commun.* **2017**, *53*, 2331.
- [33] H. Chen, F. Guo, Y. Liu, T. Huang, B. Zheng, N. Ananth, Z. Xu, W. Gao, C. Gao, *Adv. Mater.* **2017**, *29*, 1605958.
- [34] Y. Song, S. Jiao, J. Tu, J. Wang, Y. Liu, H. Jiao, X. Mao, Z. Guo, D. J. Fray, *J. Mater. Chem. A* **2017**, *5*, 1282.
- [35] D.-Y. Wang, C.-Y. Wei, M.-C. Lin, C.-J. Pan, H.-L. Chou, H.-A. Chen, M. Gong, Y. Wu, C. Yuan, M. Angell, Y.-J. Hsieh, Y.-H. Chen, C.-Y. Wen, C.-W. Chen, B.-J. Hwang, C.-C. Chen, H. Dai, *Nat. Commun.* **2017**, *8*, 14283.
- [36] S. Jiao, H. Lei, J. Tu, J. Zhu, J. Wang, X. Mao, *Carbon N. Y.* **2016**, *109*, 276.
- [37] G. Greco, D. Tatchev, A. Hoell, M. Krumrey, S. Raoux, R. Hahn, G. A. Elia, *J. Mater. Chem. A* **2018**.
- [38] S. Rothermel, P. Meister, G. Schmuelling, O. Fromm, H.-W. Meyer, S. Nowak, M. Winter, T. Placke, *Energy Environ. Sci.* **2014**, *7*, 3412.
- [39] S. Wang, K. V. Kravchyk, F. Krumeich, M. V. Kovalenko, *ACS Appl. Mater. Interfaces* **2017**, *9*, 28478.
- [40] P. Meister, G. Schmuelling, M. Winter, T. Placke, *Electrochim. Commun.* **2016**, *71*, 52.
- [41] B. Özmen-Monkul, M. M. Lerner, *Carbon N. Y.* **2010**, *48*, 3205.
- [42] G. Schmuelling, T. Placke, R. Kloepsch, O. Fromm, H.-W. Meyer, S. Passerini, M. Winter, *J. Power Sources* **2013**, *239*, 563.
- [43] I. Pócsik, M. Hundhausen, M. Koós, L. Ley, *J. Non-Cryst. Solids* **1998**, *227–230*, 1083.
- [44] A. C. Ferrari, *Solid State Commun.* **2007**, *143*, 47.
- [45] P. G. Bruce, S. A. Freunberger, L. J. Hardwick, J.-M. Tarascon, *Nat. Mater.* **2012**, *11*, 19.
- [46] S. Aladinli, F. Bordet, K. Ahlbrecht, J. Tübke, M. Holzapfel, *Electrochim. Acta* **2017**, *228*, 503.
- [47] U. Ulissi, G. A. Elia, S. Jeong, J. Reiter, N. Tsiovaras, S. Passerini, J. Hassoun, *Chem. Eur. J.* **2018**.
- [48] L. D. Reed, E. Menke, *J. Electrochim. Soc.* **2013**, *160*, A915.
- [49] U. Ulissi, G. A. Elia, S. Jeong, F. Mueller, J. Reiter, N. Tsiovaras, Y.-K. Sun, B. Scrosati, S. Passerini, J. Hassoun, *ChemSusChem* **2017**.
- [50] G. A. Elia, J.-B. Ducros, D. Sotta, V. Delhorbe, A. Brun, K. Marquardt, R. Hahn, *ACS Appl. Mater. Interfaces* **2017**, *9*, 38381.

Manuscript received: October 24, 2018

Revised manuscript received: November 10, 2018

Version of record online: December 10, 2018